Atmospheric Environment 42 (2008) 6689–6698

Contents lists available at ScienceDirect

Atmospheric Environment

journal homepage: www.elsevier.com/locate/atmosenv

α-Terpineol reactions with the nitrate radical: Rate constant and gas-phase products

Brian T. Jones [a], Jason E. Ham [b,*]

[a] Case Western Reserve University, 10900 Euclid Avenue, Cleveland, OH 44106-7078, USA
[b] Exposure Assessment Branch, Health Effects Laboratory Division, National Institute for Occupational Safety and Health, 1095 Willowdale Road, Morgantown, WV 26505, USA

ARTICLE INFO

Article history:
Received 31 December 2007
Received in revised form 7 April 2008
Accepted 7 April 2008

Keywords:
α-Terpineol
Nitrate radical
Kinetics
Reaction products
Oxygenated organic compounds

ABSTRACT

The bimolecular rate constant of $k_{NO_3^{\bullet}+\alpha\text{-terpineol}}$ $(16 \pm 4) \times 10^{-12}$ cm^3 molecule^{-1} s^{-1} was measured using the relative rate technique for the reaction of the nitrate radical ($NO_3^{\bullet}$) with α-terpineol (2-(4-methyl-1-cyclohex-3-enyl)propan-2-ol) at 297 ± 3 K and 1 atmosphere total pressure. To more clearly define part of α-terpineol's indoor environment degradation mechanism, the products of α-terpineol + $NO_3^{\bullet}$ reaction were investigated. The identified reaction products were: acetone, glyoxal (HC(=O)C(=O)H), and methylglyoxal ($CH_3C(=O)C(=O)H$). The use of derivatizing agents *O*-(2,3,4,5,6-pentafluorobenzyl)-hydroxylamine (PFBHA) and *N*,*O*-bis(trimethylsilyl) trifluoroacetamide (BSTFA) were used to propose the other major reaction products: 6-hydroxyhept-5-en-2-one, 4-(1-hydroxy-1-methylethyl)-1-methyl-2-oxocyclohexyl nitrate, 5-(1-hydroxy-1-methylethyl)-2-oxocyclohexyl nitrate, 1-formyl-5-hydroxy-4-(hydroxymethyl)-1,5-dimethylhexyl nitrate, and 1,4-diformyl-5-hydroxy-1,5-dimethylhexyl nitrate. The elucidation of these products was facilitated by mass spectrometry of the derivatized reaction products coupled with plausible α-terpineol + $NO_3^{\bullet}$ reaction mechanisms based on previously published volatile organic compound + $NO_3^{\bullet}$ gas-phase mechanisms. The additional gas-phase products (2,6,6-trimethyltetrahydro-2*H*-pyran-2,5-dicarbaldehyde and 2,2-dimethylcyclohexane-1,4-dicarbaldehyde) are proposed to be the result of cyclization through a reaction intermediate.

Published by Elsevier Ltd.

1. Introduction

The nitrate radical ($NO_3^{\bullet}$) has been identified as the main reactive species in the nighttime outdoor environment and has been hypothesized to be present in indoor environments. In the outdoor environment, NO that is present in the troposphere from biogenic and anthropogenic sources can react with ozone to produce NO_2 which can then react further with ozone to produce the nitrate radical as seen in Reactions (1) and (2).

$$NO + O_3 \rightarrow NO_2 + O_2 \quad (1)$$

$$NO_2 + O_3 \rightarrow NO_3^{\bullet} + O_2 \quad (2)$$

In the indoor environment, given the absence of sunlight (due to photochemical decomposition of $NO_3^{\bullet}$), Reaction (2) could be of considerable importance, especially in areas where there is little or no light such as HVAC ducts, spaces above dropped ceilings, or below raised floors (Weschler and Shields, 1997). Given this, Weschler et al. (1994) have measured indoor O_3 and NO_2 concentrations (25 and 30 ppb, respectively) in a commercial building in Burbank, CA, during mid-afternoon periods between April and October, which given the rate constant of reaction (Reaction (2))

* Corresponding author. Tel.: +1 304 285 6214; fax: +1 304 285 6041.
E-mail address: bvo2@cdc.gov (J.E. Ham).

1352-2310/$ – see front matter Published by Elsevier Ltd.
doi:10.1016/j.atmosenv.2008.04.017

($k_2 = 7.87 \times 10^{-7}$ ppb^{-1} s^{-1}) generates NO_3• at ~2 ppb h^{-1}. Ozone can be introduced indoors by outdoor-to-indoor ventilation or produced by mechanical means (i.e. laser printers, copiers). NO_2 can also be brought in by ventilation or produced by combustion sources (i.e., unvented combustion appliances, e.g. gas stoves, vented appliances with defective installations, welding, and tobacco smoke) (EPA, 2006). These concentrations of O_3 and NO_2 are expected to be large enough for significant production of nitrate radicals. Although nitrate radical concentrations have not been measured in indoor environments, evidence of the radical's existence has been inferred from the significant concentrations of nitric acid (HNO_3) (up to 0.84 ppb) found in indoor environments (Brauer et al., 1991; Weschler et al., 1992). One caveat to consider is that the reaction between O_3 and NO_2 is slow; however, when concentrations of these species are elevated and air exchange rates are moderate to low then this reaction can be important.

Nitrate radical reactions with alkenes can be considerably fast when compared to a typical air exchange of 0.6 h^{-1} (Wilson et al., 1996). For example, pseudo-first order rate constants of limonene, terpinolene, and α-terpinene have been calculated to be 1.1, 8.6, and 16 h^{-1}, respectively (Nazaroff and Weschler, 2004). Additionally, alkene + NO_3• reactions lead to a number of oxygenated products such as: aldehydes, ketones, dicarbonyls, and organic nitrates (e.g. alkyl nitrates, peroxyacyl nitrates (PANs), hydroxynitrates, dinitrates). All of these oxygenated organic compounds have the potential to induce a respiratory response. For example, local lymph node assay (LLNA) results showed the dicarbonyls (methylglyoxal and diacetyl) to be irritants and sensitizers with EC3 values ranging from 0.42 to 1.9% (Anderson et al., 2007). Although little data exists on the toxicology of other organic nitrates, they are possible carcinogens and investigating their formation in indoor environments will be important for assessing worker health (Finlayson-Pitts and Pitts, 2000).

Cleaning and air freshening are common activities which can introduce many volatile organic compounds (VOCs) or semi-VOCs into the indoor environment. One such compound used in these activities is α-terpineol (2-(4-methyl-1-cyclohex-3-enyl)propan-2-ol) (see Structure 1), a significant component of pine oil cleaners. In the work presented here, the α-terpineol + NO_3• rate constant has been measured using the relative rate method. Some of the products of this reaction are also reported. Neither the NO_3• rate constant, nor the respective reaction mechanisms for α-terpineol + NO_3• have been reported previously.

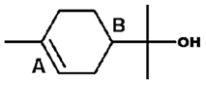

2. Experimental methods

2.1. Apparatus and materials

Experiments to measure the gas-phase rate constant of the NO_3• + 2-(4-methyl-1-cyclohex-3-enyl)propan-2-ol (α-terpineol, Structure 1) reaction were conducted with a previously described apparatus (Forester et al., 2007; Ham et al., 2006). A brief description is provided here. Reactants were introduced and samples were withdrawn through a 6.4 mm Teflon® Swagelok fitting attached to a 65 L Teflon® film chamber. Compressed air from the National Institute for Occupational Safety and Health (NIOSH) facility was passed through anhydrous $CaSO_4$ (Drierite, Xenia, OH) and molecular sieves (Drierite, Xenia, OH) to remove both moisture and organic contaminants. This dry compressed air was added as a diluent to the reaction chambers and measured with a 0–100 L min^{-1} mass flow controller (MKS, Andover, MA). Analysis of this treated compressed air by gas chromatography/mass spectrometry revealed that if contaminants were present they would be below a part per trillion range. The treated compressed air was also analyzed for nitric oxide (NO) using a Thermo Electron Model 42i NO-NO_2-NO_x Analyzer (Waltham, MA). The filler system was equipped with a syringe injection port facilitating the introduction of both liquid and gaseous reactants into the chambers with the flowing air stream. All reactant mixtures and calibration standards were generated by this system.

All reaction kinetic samples were quantitatively monitored using an Agilent (Palo Alto, CA) 6890 gas chromatograph with a 5973 mass selective detector (GC/MS) and Agilent ChemStation software. Gas samples were cryogenically collected employing an Entech 7100 (Simi Valley, CA) sampling system utilizing the following trap and temperature parameters: 50 mL of chamber contents were collected onto Trap 1 (packed silanized glass beads) at −150 °C. After sample collection, Trap 1 was heated to 230 °C and the sample transferred under a flow of ultra-high purity helium (UHP He) onto Trap 2 (packed silanized glass beads) cooled to −30 °C. Trap 2 was then heated to 180 °C and the sample transferred under a UHP He flow onto Trap 3, a silanized 0.53 mm i.d. tube cooled to −160 °C which was subsequently heated to 220 °C to inject the sample onto an Rtx-VRX (Restek, Bellefonte, PA) GC column (0.25 mm i.d., 30 m long, 1.4 μm film thickness). These series of cryogenic trap manipulations reduced the background water level, ensured consistency of replicate samples, and improved the chromatograph peak shapes. The reduction in background water levels is accomplished by gentle heating (40 °C) with helium flow on each of the traps along with careful timing of cooling the next trap for collection. The GC temperature program used was: initial temperature of 45 °C held for 8 min after sample injection then increased 10 °C min^{-1} to 220 °C and held for 4 min. The Agilent 5973 mass selective detector was tuned using perfluorotributylamine (FC-43). Full-scan electron impact (EI) ionization spectra were collected from m/z 35 to 650. Preliminary compound identifications from the Agilent 6890/5973 GC/MS data sets were made by searching the NIST 98 Mass Spectral Library.

Identification of reaction products was made using *O*-(2,3,4,5,6-pentafluorobenzyl)hydroxylamine (PFBHA) to derivatize carbonyl products, while alcohol and carboxylic acid products were derivatized using PFBHA and *N,O*-bis (trimethylsilyl)trifluoroacetamide (BSTFA) (Yu et al., 1998). Experimental methods for reaction product identification were similar to methods used for kinetic experiments,

except the reference compound was excluded from the reaction mixture. An additional port was added to the Teflon chamber to facilitate the injection of ozone.

Derivatized reaction products were analyzed using a Varian (Palo Alto, CA) 3800/Saturn 2000 GC/MS system operated in both the EI and CI modes (Yu et al., 1998). Compound separation was achieved by a J&W Scientific (Folsom, CA) DB-5MS (0.32 mm i.d., 30 m long, 1 μm film thickness) column and the following GC oven parameters: 60 °C for 1 min, then 20 °C min^{-1} to 170 °C, then 3 °C min^{-1} to 280 °C and held for 5 min.

Samples were injected in the splitless mode, and the GC injector was returned to split mode one min after sample injection, with the following injector temperature parameters: 60 °C for 1 min then 180 °C min^{-1} to 250 °C and held to the end of the chromatographic run (Yu et al., 1998). The Saturn 2000 ion trap mass spectrometer was tuned using FC-43. Full-scan EI ionization spectra were collected from m/z 40 to 650. Acetonitrile was the chemical ionization reagent used for all CI spectra. When possible, commercially available samples of the identified products were derivatized and subsequently analyzed to verify matching ion spectra and chromatographic retention times.

Nitrate radicals were generated by the thermal decomposition of N_2O_5 using a similar method as described by Atkinson et al. (1988, 1984). N_2O_5 (solid) kept at −85 °C was heated and allowed to transfer to an evacuated 2 L collection bottle until pressure was between 0.2 and 0.6 Torr. The collection bottle was then pressurized with ultra-high purity nitrogen up to 1000 Torr and connected to the reaction chamber via a Teflon® shut-off valve. The valve to the collection bottle and the chamber shut-off valve were opened and the system was allowed to equilibrate for 10 s.

$$N_2O_5 \overset{M}{\rightleftarrows} NO_3^{\bullet} + NO_2 \quad (3)$$

All compounds were used as received and had the following purities: from Sigma-Aldrich (Milwaukee, WI): 3-carene (90%), 2-(4-methyl-1-cyclohex-3-enyl)propan-2-ol (α-terpineol) (90%), 2-carene (97%), acetonitrile (99.93%), *N,O*-bis(trimethylsilyl)trifluoroacetamide (BSTFA) (99%), *O*-(2,3,4,5,6-pentafluorobenzyl) hydroxylamine hydrochloride (PFBHA) (98+%), glyoxal (40% in water) and methylglyoxal (40% in water); from Fisher Scientific (Fairlawn, NJ): methanol (99%) and hydrogen peroxide (30%). Nitrogen dioxide as a 5% mixture in nitrogen and ultra-high purity oxygen were obtained from Butler Gases (Morrisville, PA). Helium (UHP grade), the carrier gas, was supplied by Amerigas (Sabraton, WV) and used as received. Experiments were carried out at 297 ± 3 K and 1 atmosphere pressure.

2.2. Experimental procedures

The experimental procedures for determining the α-terpineol + $NO_3^{\bullet}$ reaction kinetics were similar to those described previously (Forester et al., 2007; Ham et al., 2006; Wells, 2005).

$$\alpha\text{-terpineol} + NO_3^{\bullet} \xrightarrow{k_{NO_3+\alpha\text{-terpineol}}} \text{Products} \quad (4)$$

$$\text{Reference} + NO_3^{\bullet} \xrightarrow{k_{Ref}} \text{Products} \quad (5)$$

The rate equations for Reactions (1) and (2) are combined and integrated, resulting in the following equation:

$$\ln\left(\frac{[\alpha\text{-terpineol}]_0}{[\alpha\text{-terpineol}]_t}\right) = \frac{k_{NO_3+\alpha\text{-terpineol}}}{k_{Ref}} \ln\left(\frac{[Ref]_0}{[Ref]_t}\right) \quad (6)$$

If reaction with $NO_3^{\bullet}$ is the only removal mechanism for α-terpineol and reference, a plot of $\ln([\alpha\text{-terpineol}]_0/[\alpha\text{-terpineol}]_t)$ versus $\ln([Ref]_0/[Ref]_t)$ yields a straight line with an intercept of zero. Multiplying the slope of this linear plot by k_{Ref} yields $k_{NO_3^{\bullet}+\alpha\text{-terpineol}}$ (Fig. 1). The $NO_3^{\bullet}$ rate constant experiments for α-terpineol employed the use of two reference compounds: 3-carene and 2-carene. The use of two different reference compounds with different $NO_3^{\bullet}$ rate constants aids to ensure the accuracy of the α-terpineol/$NO_3^{\bullet}$ rate constant and demonstrates that other reactions are not removing α-terpineol.

For the α-terpineol/$NO_3^{\bullet}$ kinetic experiments the typical concentrations of the pertinent species in the 65 L Teflon chamber were 0.5–0.9 ppm ($1.2–2.2 \times 10^{13}$ molecule cm^{-3}) α-terpineol, 0.5–0.9 ppm ($1.2–2.2 \times 10^{13}$ molecule cm^{-3}) reference, 0.2–0.6 Torr of N_2O_5, and 6 ppb (1.4×10^{11} molecule-cm^{-3}) NO in air. The gas-phase mixtures were allowed to reach equilibrium before initial species concentration ($[X]_0$) samples were collected. The total ion chromatogram (TIC) from the Agilent 5973 mass selective detector was used to determine α-terpineol and reference concentrations.

Derivatization of the carbonyl reaction products was initiated by flowing 15–25 L of chamber contents at 3.8 L min^{-1} through an impinger containing 4 mL of acetonitrile and 250 μL of 0.02 M PFBHA in acetonitrile to derivatize the carbonyl reaction products to oximes (Yu et al., 1998) with no effort to prevent acetonitrile evaporation during sample collection. The sample was removed from

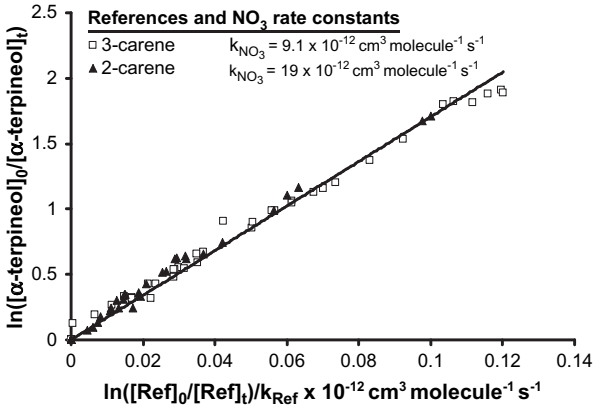

Fig. 1. (R)-2-(4-methyl-3-cyclohexenyl)isopropanol (α-terpineol) relative rate plot with 3-carene (□) and 2-carene (▲) as reference compounds. The $NO_3^{\bullet}$ + α-terpineol rate constant, $k_{NO_3^{\bullet}+\alpha\text{-terpineol}}$, was measured to be $(16 \pm 0.2) \times 10^{-12}$ cm^3 $molecule^{-1}$ s^{-1}.

the impinger and allowed to react for a 24–48 h time period in the dark. The reacted solutions were gently blown to dryness with UHP N_2, reconstituted with 100 μL of methanol, and then 1 μL of the reconstituted solution was injected onto the Varian 3800/Saturn 2000 GC/MS system. The derivatization of hydroxy groups (either alcohol or carboxylic acid) was achieved by subsequent reconstitution of the dried PFBHA oximes-addition with 150 μL of commercially available BSTFA. These PFBHA/BSTFA solutions were heated to approximately 60 °C for 45 min to complete the silylation and then 1 μL of the solution was injected into the Varian 3800/Saturn 2000 GC/MS system (Forester et al., 2007).

3. Results

3.1. α-Terpineol/NO_3• reaction rate constant

The NO_3• rate constant for α-terpineol (Structure 1) was obtained using the relative rate method described above. The plot of a modified version of equation (6) is shown in Fig. 1. The $\ln([Ref]_0/[Ref]_t)$ term is divided by the respective reference rate constant (3-carene $(9.1 \pm 2.3) \times 10^{-12}$ cm^3 $molecule^{-1}$ s^{-1} and 2-carene $(19 \pm 5) \times 10^{-12}$ cm^3 $molecule^{-1}$ s^{-1}) (Atkinson and Arey, 2003) and multiplied by 10^{-12} cm^3 $molecule^{-1}$ s^{-1}, resulting in a unitless number. This yields a slope that is equal to the NO_3•/α-terpineol rate constant, $k_{NO_3\bullet+\alpha\text{-terpineol}}$, divided by 10^{-12} cm^3 $molecule^{-1}$ s^{-1}. This modification allows for a direct comparison of the two reference compound/α-terpineol data sets. The slope of the line shown in Fig. 1 yields an NO_3• bimolecular rate constant, $k_{NO_3\bullet+\alpha\text{-terpineol}}$, of (16 ± 0.2) 10^{-12} cm^3 $molecule^{-1}$ s^{-1}. The use of 3-carene and 2-carene as references resulted in NO_3• + α-terpineol bimolecular rate constants of (16 ± 0.3) and (18 ± 0.3) 10^{-12} cm^3 $molecule^{-1}$ s^{-1}, respectively. The data points at the origin are experimental points before NO_3•-addition, $t = 0$, data showed no detectable loss of α-terpineol or reference. The error in the rate constant stated above is the 95% confidence level from the random uncertainty in the slope. Incorporating the uncertainties associated with the reference rate constants (±25% for 3-carene and 2-carene) used to derive the α-terpineol/NO_3• rate constant yields a final value for $k_{NO_3\bullet+\alpha\text{-terpineol}}$, of $(16 \pm 4) \times 10^{-12}$ cm^3 $molecule^{-1}$ s^{-1} (Atkinson and Arey, 2003). The α-terpineol/NO_3• rate constant, $k_{NO_3\bullet+\alpha\text{-terpineol}}$, has not been previously reported.

3.2. α-Terpineol/NO_3• reaction products

The reaction products observed from the α-terpineol/NO_3• (hydrogen abstraction or NO_3•-addition to the carbon–carbon double bond) are listed in Table 1. The α-terpineol/NO_3• reaction products observed and positively identified using the pure compound for verification by derivatization were: acetone, glyoxal (HC(=O)C(=O)H), and methylglyoxal (CH_3C(=O)C(=O)H). Structures and ions used to identify these compounds are listed in Table 1. Elucidation of the other major reaction products (also listed in Table 1) were facilitated by mass spectrometry of the derivatized reaction product coupled with plausible α-terpineol/NO_3• reaction mechanisms based on previously published volatile organic compound/NO_3• gas-phase reaction as described below (Atkinson and Arey, 2003; Espada et al., 2005; Finlayson-Pitts and Pitts, 2000; Skov et al., 1992; Spittler et al., 2006; Weschler and Shields, 1997).

Derivatization of nonsymmetric carbonyls using PFBHA or PFBHA/BSTFA typically resulted in multiple chromatographic peaks due to stereoisomers of the oximes. Identification of multiple peaks of the same oxime compound is relatively simple since the mass spectra for each chromatographic peak of a particular oxime are almost identical (Yu et al., 1998). In most cases, the m/z 181 ion relative intensity for the chromatographic peaks due to α-terpineol + NO_3• reaction product oximes was the base peak in the mass spectrum and was used to generate selected ion chromatograms (Yu et al., 1998). The mass spectra of compounds that were additionally derivatized with BSTFA contained m/z 73 ions from the $[Si(CH_3)_3]^+$ fragments (Yu et al., 1998). A chromatogram displaying the latter portion of the GC run (29–48 min) in which organic nitrate products were observed is shown in Fig. 2. This figure shows the chromatograms obtained from α-terpineol + air only, NO_3• only in the reaction chamber, and α-terpineol + NO_3•. Several peaks were observed in the NO_3• only experiments, but were disregarded as they did not interfere with the reported reaction products. The product data are described below.

The following chronological chromatographic retention time results and mass spectra data were observed utilizing PFBHA or PFBHA/BSTFA derivatization and the Varian 3800/Saturn 2000 GC/MS system. The reaction products' chromatographic peak areas were a function of the initial α-terpineol concentration and were observed only after NO_3• initiation of α-terpineol/methanol/air mixtures. Derivatization experiments performed in the absence of α-terpineol, but in the presence of all other chemicals in the reaction chamber (NO_3•/air) did not result in any of the data reported below except for small amounts (as noted by chromatographic peak areas) of methylglyoxal and glyoxal. However, the glyoxal and methylglyoxal oxime peak areas increased significantly by a factor of 5 and 16, respectively, with α-terpineol + NO_3• indicating that methylglyoxal and glyoxal are likely products of the reaction.

3.3. Acetone 7.8 min

The chromatographic peak for the oxime observed at 7.8 min has been described previously (Forester et al., 2007).

3.4. Oxime at retention time 16.4 min

The oxime observed with a chromatographic retention time of 16.4 min had ions of m/z (relative intensity): 79 (70–75%), 107 (70–75%), 181 (100%), 195 (10–15%), 277 (10–20%), and 306 (5–10%). Using acetonitrile for chemical ionization, an M + 1 ion of m/z 306 was observed for the PFBHA-derivatized sample. A proposed reaction product assignment of 4-methylcyclohex-3-en-1-one was based on observed data (Wells, 2005).

Table 1
Proposed molecular structures of α-terpineol + $NO_3^•$ reaction products

R.t (min)	Name	Molecular weight (amu)	Structure	Cl ions observed
7.8	Acetone	58		254
16.4	4-Methylcyclohex-3-en-1-one	110	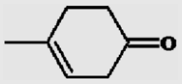	306
19.6	6-Hydroxyhept-5-en-2-one	128	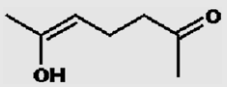	324
24.1 24.4	Glyoxal	58	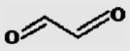	449
24.5 25.5	Methylglyoxal	72		463
30.7 31.8	4-(1-Hydroxy-1-methylethyl)-1-methyl-2-oxocyclohexyl nitrate	231	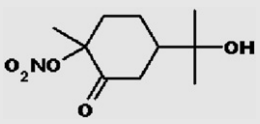	380
34.2	5-(1-Hydroxy-1-methylethyl)-2-oxocyclohexyl nitrate	217	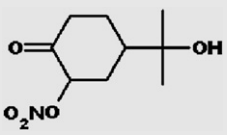	412
37.7	2,6,6-Trimethyltetrahydro-2*H*-pyran-2,5-dicarbaldehyde	184	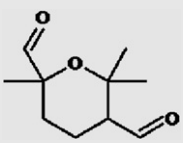	574,556
38.3 38.5 39.2 39.4	2,2-Dimethylcyclohexane-1,4-dicarbaldehyde	168	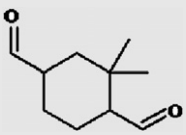	559,364
40.8	1-Formyl-5-hydroxy-4-(hydroxymethyl)-1,5-dimethylhexyl nitrate	249	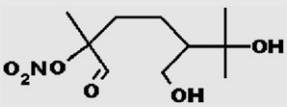	399
41.8 42.8	1,4-Diformyl-5-hydroxy-1,5-dimethylhexyl nitrate	247	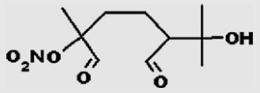	559,364

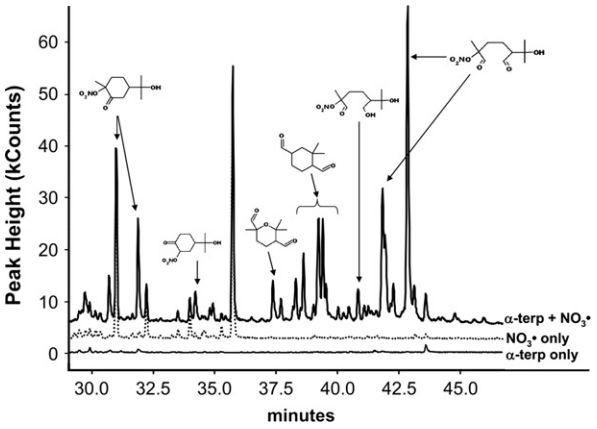

Fig. 2. Overlayed chromatograms of α-terpineol only (lower solid line), $NO_3^•$ only (dotted line), and α-terpineol + $NO_3^•$ (upper solid line) in the reaction chamber. Data was offset for clarity.

3.5. Oxime at retention time 19.6 min

The oxime observed with a chromatographic retention time of 19.6 min had ions of *m*/*z* (relative intensity): 107 (40–50%), 126 (40–45%), 181(75–85%), 288 (75%), 305 (100%), and 324 (25–35%). Using acetonitrile for chemical ionization, an M + 1 ion of *m*/*z* 324 was observed for the PFBHA-derivatized sample. A proposed reaction product assignment of 6-hydroxyhept-5-en-2-one was based on observed data.

PFBHA/BSTFA derivatization of the oxime at 19.6 showed a chromatographic peak shift in retention time to 22.3 min. Using acetonitrile for chemical ionization, an M + 1 ion of *m*/*z* 396 was observed. BSTFA adds *m*/*z* 72 to the PFBHA-derivatized oxime, indicating the presence of an OH group. This data was used to further verify the proposed assignment of the 19.6 min peak (Wells, 2005).

3.6. Glyoxal (HC(=O)C(=O)H)

The chromatographic peaks for the oxime observed at 24.1 and 24.4 min have been described previously (Forester et al., 2007).

3.7. Methylglyoxal ($CH_3C(=O)C(=O)H$)

The chromatographic peaks for the oxime observed at 24.5 and 25.5 min have been described previously (Forester et al., 2007).

3.8. Oxime at retention times 30.7 and 31.8 min

The oxime observed at retention 30.7 and 31.8 min had ions of *m*/*z* (relative intensity): 43 (15–20%), 97 (20%), 181 (100%), 321 (5–10%), 362 (60–65%), 379 (10%), see Fig. 3. Using acetonitrile for chemical ionization, an M + 1 ion of *m*/*z* 380 was observed. A proposed reaction product assignment of 4-(1-hydroxy-1-methylethyl)-1-methyl-2-oxocyclohexyl nitrate was based on observed data. No peak was observed in PFBHA/BSTFA experiments.

3.9. Oxime at retention time 34.2 min

The oxime observed at a retention time of 34.2 min had ions of *m*/*z* (relative intensity): 43 (15–20%), 77 (20%), 128 (20–25%), 144 (50–60%), 181 (100%), 325 (30–35%), 353 (15%). Using acetonitrile for chemical ionization, an M + 1 ion of *m*/*z* 412 was observed. A proposed reaction product assignment of 5-(1-hydroxy-1-methylethyl)-2-oxocyclohexyl nitrate was based on observed data. No peak was observed in PFBHA/BSTFA experiments.

3.10. Oxime at retention time 37.7 min

The oxime observed at a retention time of 37.7 min had ions of *m*/*z* (relative intensity): 81 (15–20%), 108 (75%), 136 (15%), 181 (100%), 334 (10%), 375 (90%). Using acetonitrile for chemical ionization, an M + 1 ion of *m*/*z* 573 was observed. A proposed reaction product assignment of 2,6,6-trimethyltetrahydro-2*H*-pyran-2,5-dicarbaldehyde was based on observed data.

3.11. Oxime at retention times 38.3, 38.5, 39.2 and 39.4 min

The oxime observed at retention times 38.3, 38.5, 39.2, and 39.4 min had ions of *m*/*z* (relative intensity): 166 (25–40%), 181 (100%), 266 (10–15%), 320 (10–20%), 347 (5–10%), 361 (40–50%), 377 (20–30%). Using acetonitrile for chemical ionization, an M + 1 ion of *m*/*z* 559 was observed. A proposed reaction product assignment of

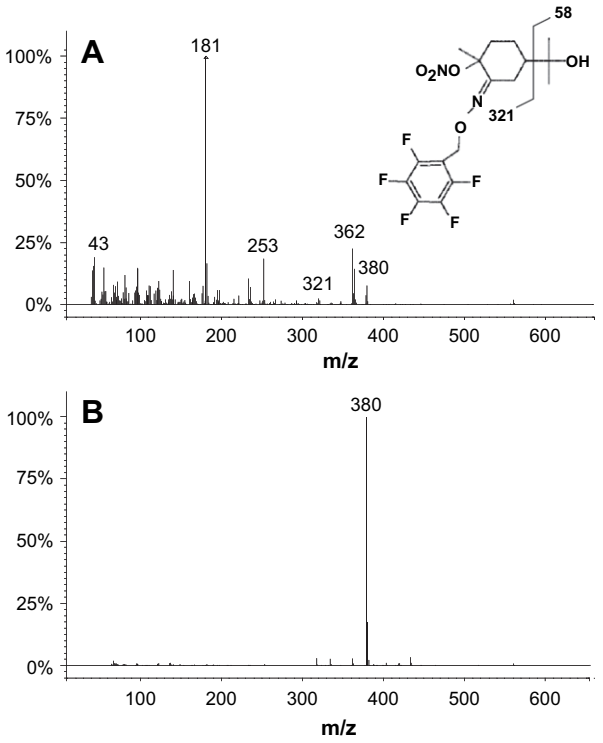

Fig. 3. PFBHA-derivatized product (4HMON) of α-terpineol + $NO_3^•$ (30.7 min): (A) electron ionization spectrum and (B) acetonitrile chemical ionization spectrum.

2,2-dimethylcyclohexane-1,4-dicarbaldehyde was based on observed data.

3.12. Oxime at retention time 40.8 min

The oxime observed at a retention time of 40.8 min had ions of m/z (relative intensity): 181 (100%), 266 (10%), 334 (15–20%), 362 (70–75%), 398 (5%). Using acetonitrile for chemical ionization, an M + 1 ion of m/z 398 was observed. A proposed reaction product assignment of 1-formyl-5-hydroxy-4-(hydroxymethyl)-1,5-dimethylhexyl nitrate was based on observed data.

PFBHA/BSTFA derivatization of the oxime at 40.8 min showed a chromatographic peak shift in retention time to 31.6 min. Using acetonitrile for chemical ionization, an M + 1 ions of m/z 398(100%) and 471 (15%) were observed. This data was used to further verify the proposed assignment of the 40.8 min peak.

3.13. Oxime at retention times 41.8 and 42.8 min

The oxime observed at retention times of 41.8 and 42.8 min had ions of m/z (relative intensity): 59 (20%), 181 (100%), 266 (20%), 278 (10%), 306 (10%), 364 (55–60%), 379 (25–30%), 517 (5%), 543 (5%), 559 (5%), see Fig. 4. Using acetonitrile for chemical ionization, an M + 1 ions of m/z 559 (50%) and 364 (100%) were observed. A proposed reaction product assignment of 1,4-diformyl-5-hydroxy-1,5-dimethylhexyl nitrate was based on observed data.

PFBHA/BSTFA derivatization of the oxime at 41.8 and 42.8 min showed a chromatographic peak shift in retention time to 44.1 min. Electron ionization (EI) spectra of these peaks showed ions at m/z (relative intensity): 73 (75%), 131 (100%), 181 (55–60%), 361 (50%), 377 (20%), 451 (15%), 467 (5%), 633 (3%). Chemical ionization spectra did not show an ion m/z of 647 indicating PFBHA/BSTFA derivatization. This could be due to lower sensitivity at the end of the mass spectral scan. Nevertheless, EI data was used to further verify the proposed assignment of the 40.8 min peak.

4. Discussion

The nitrate radical (NO_3•) can react with α-terpineol by H-atom abstraction or NO_3•-addition to carbon–carbon double bonds (Finlayson-Pitts and Pitts, 2000; Spittler et al., 2006; Weschler and Shields, 1997). Structure 1 shows the most likely sites for these nitrate radical reactions. The measured value reported here $(16 \pm 4) \times 10^{-12}$ cm^3 molecule^{-1} s^{-1} is slower than the previously reported OH• reaction, $k_{OH\bullet + \alpha\text{-terpineol}}$ of $(190 \pm 50) \times 10^{-12}$ cm^3 molecule^{-1} s^{-1} (Wells, 2005). This value can also be compared to the calculated value of 9.4×10^{-12} cm^3 molecule^{-1} s^{-1} which is approximately 1.7 times slower than the measured value (Atkinson, 2000).

For the α-terpineol + NO_3• reaction the experimental parameters were set to minimize side reactions and highlight the NO_3• hydrogen abstraction and/or NO_3•-addition. Furthermore, experiments were done with α-terpineol + NO_2 (byproduct of N_2O_5 thermal degradation) to determine if products were from these reactions. No reaction products observed here were due to NO_2 chemistry. The possible mechanistic steps leading to product formation are described below.

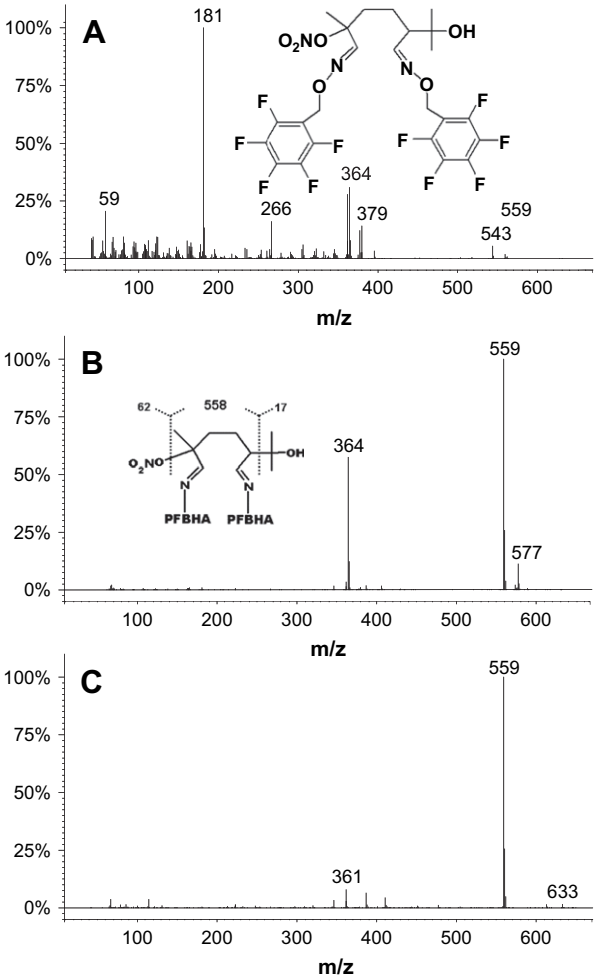

Fig. 4. PFBHA-derivatized product (DHDN) of α-terpineol + NO_3• (41.8 min): (A) electron ionization spectrum, (B) acetonitrile chemical ionization spectrum, and (C) PFBHA/BSTFA derivatized product using acetonitrile chemical ionization.

4.1. Hydrogen abstraction by NO_3•

Hydrogen abstraction of the tertiary hydrogen of α-terpineol can lead to the formation of acetone and 4-methylcyclohex-3-en-1-one, as seen in Fig. 5. Abstraction of this hydrogen produces two products: an α-terpineol radical (**I**) and HNO_3. Structure (**I**) can then dissociate into structure (**II**) via O_2-addition and the radical, $(CH_3)_2C(\bullet)OH$. The 2-propanol radical will then be stabilized by loss of H and formation of acetone. The peroxy radical (structure (**II**)) can further react with NO to form NO_2 and structure (**III**). This structure is then stabilized to 4-methylcyclohex-3-en-1-one. Further confirmation of the mechanism of acetone and this product is supported by the observation of both in the similar gas-phase reaction of α-terpineol + OH• (Wells, 2005).

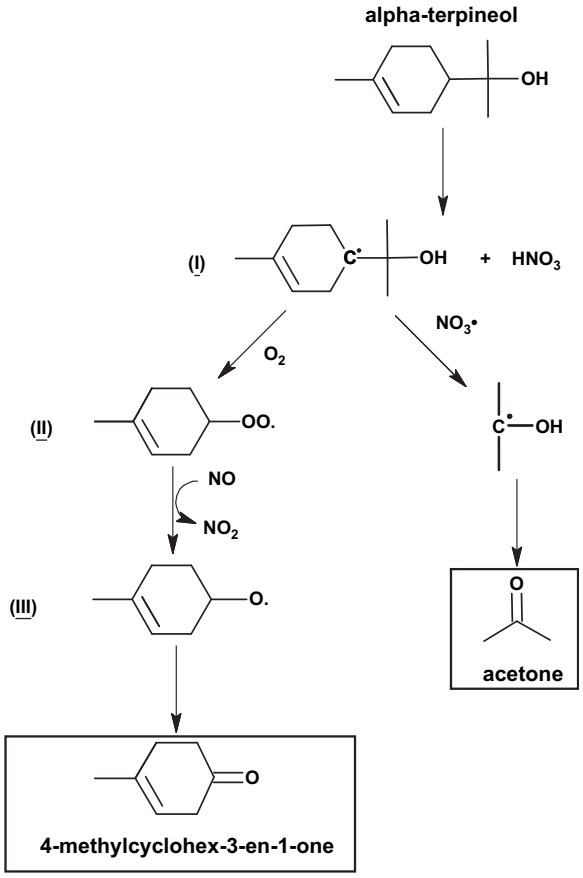

Fig. 5. Proposed reaction mechanism for the hydrogen abstraction of the tertiary hydrogen of α-terpineol by NO_3•.

4.2. NO_3•-addition to carbon–carbon double bond

At present, the mechanistic pathways for the formation of the other proposed products that were observed in the gas-phase reaction of α-terpineol + NO_3• are speculative. However, it is possible to propose a reaction scheme as shown in Fig. 6. Initially, the nitrate radical can add to either side of the carbon–carbon double bond leading to the formation of structures (**IV**) and (**V**). Structure (**IV**), through multiple reaction steps, can produce two of the observed products: 6-hydroxyhept-5-en-2-one and 5-(1-hydroxy-1-methylethyl)-2-oxocyclohexyl nitrate (5HMON). 6-hydroxyhept-5-en-2-one can be generated via structure (**IV**) by loss of NO_3•, and ring opening. The radicals formed on the carbons on either side of the carbon–carbon double bond go through O_2-addition and isomerization of adjacent hydrogens to produce the ketone–alcohol. This product was not unexpected due to the similar gas-phase chemistry observed with α-terpineol + OH• (Wells, 2005). The organic nitrate (5HMON) that can be generated by structure (**IV**) is produced by O_2-addition to the carbon radical to form the peroxide with subsequent reaction with NO. Stabilization of the new carbonyl results in ejection of $-CH_3$ and formation of 5-(1-hydroxy-1-methylethyl)-2-oxocyclohexyl nitrate. Further confirmation of this product is observed in the mass spectrum of 34.2 min oxime by the expected loss of the 2-propanol moiety (m/z 58) and observance of an ion at m/z 353.

Structure (**V**), also through multiple reaction steps, can lead to the production of three other observed products: 4-(1-hydroxy-1-methylethyl)-1-methyl-2-oxocyclohexyl nitrate (4HMON), 1-formyl-5-hydroxy-4-(hydroxymethyl)-1,5-dimethylhexyl nitrate (FHDN), and 1,4-diformyl-5-hydroxy-1,5-dimethylhexyl nitrate (DHDN). 4HMON can be generated from structure (**V**) by O_2-addition to the carbon radical to form the peroxy radical. Subsequent reaction with NO to form NO_2 and stabilization of the carbonyl leads to the observed nitrate product. Further confirmation to the proposed identification of this product is observed in the mass spectra of the 30.7 and 31.8 min oxime by the expected loss of the 2-propanol moiety (m/z 58) and observance of an ion at m/z 321, see Fig. 3. Additionally, the observance of an ion at m/z 362 indicates the loss of OH. FHDN, like 4HMON, is produced from structure (**V**) by O_2-addition with subsequent reaction with NO. The radical can then be stabilized to form the carbonyl by removing the adjacent hydrogen causing the ring to open which leads to structure (**VI**). Addition of O_2 and subsequent NO reaction produces the reaction intermediate, structure (**VII**). This intermediate can add hydrogen to generate the carbonyl–alcohol (FHDN) or stabilize the carbonyl to form the other organic nitrate (DHDN). The proposed identity of FHDN was made by observance of the ion at m/z 398 which may be produced by the loss of NO_2 (m/z 46). This loss has been commonly observed in mass spectra of alkyl and arylalkyl nitrates (Kames and Schurath, 1993; Woidich et al., 1999). Identification of DHDN was based on the observance of the ion at m/z 559 which can be due to loss of NO_3 (m/z 62) and OH (m/z 17). Additionally, the observance of an ion at m/z 364 indicates double derivatization by loss of 195 (PFBHA group). Due to the close proximity of these groups in its stabilized structure, it is not unreasonable that their interaction leads to their loss and production of a stable ion in the gas-phase.

The final two reaction products that were observed from α-terpineol + NO_3• were: 2,6,6-trimethyltetrahydro-2H-pyran-2,5-dicarbaldehyde (TPD) and 2,2-dimethylcyclohexane-1,4-dicarbaldehyde (DCD). These two products are likely secondary products from the organic nitrate (DHDN) as seen in the proposed mechanistic scheme, see Fig. 7. Rearrangement of DHDN to its more stable structure can place the NO_3 group and the OH in close proximity. Interaction of these groups leads to OH and NO_2 or NO_3 loss. The subsequent energy-rich intermediates can through annelation form the 6-membered ring structures, TPD and DCD. These types of cyclization are analogous to radical mediated ring closure mechanisms discussed in published literature (Rheault and Sibi, 2003; Semikolenov et al., 2002; Shu et al., 1997).

A number of other oxygenated organic compounds were expected from the reaction of α-terpineol + NO_3•, but were not observed (see Fig. 6) including: an α-terpineol epoxide (**1**), an α-terpineol dinitrate (**2**), a dicarbonyl–nitrate compound (**3**), and two other dicarbonyl compounds (**4**) and (**5**). The α-terpineol epoxide may be produced in the gas-phase; however, since this product cannot be derivatized with PFBHA it is difficult to verify its presence using the

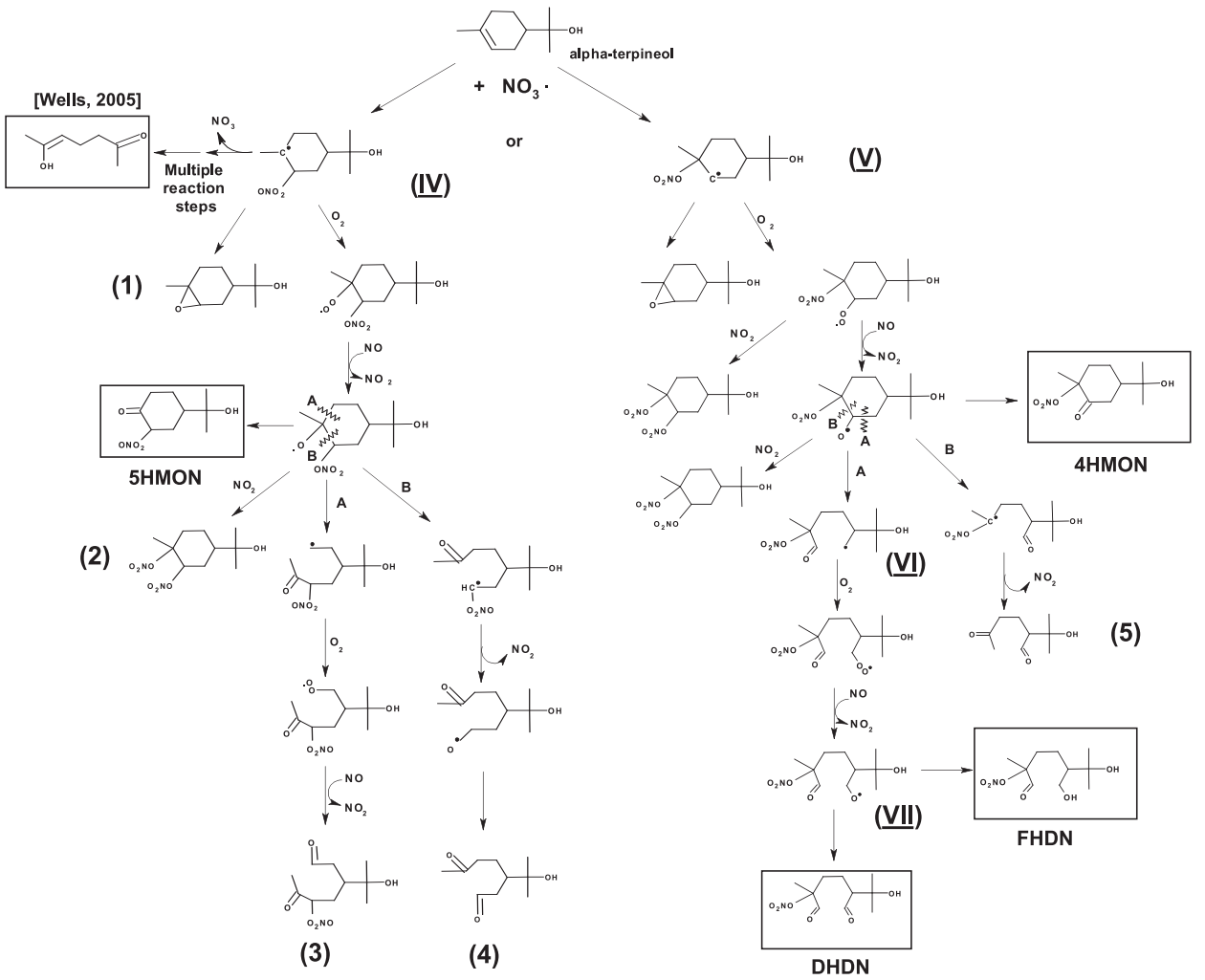

Fig. 6. Proposed reaction mechanism for NO_3•-addition to the carbon–carbon double bond of α-terpineol.

described detection methods. Experiments using BSTFA derivatization only did not show any of the listed products. These possible reaction products may be undetected due to very low yields or loss to the Teflon bag surface.

4.3. Indoor nitrate radical chemistry

Approximate indoor environment concentrations of the nitrate radical (2.46×10^7 molecules cm^{-3}) have been previously estimated by Sarwar et al. (2002). Using the α-terpineol + NO_3• rate constant reported here, a pseudo-first order rate constant (k') of 1.4 h^{-1} was determined. A comparison of this value to a typical indoor air exchange rate of 0.6 h^{-1} (Wilson et al., 1996) suggests that NO_3 radical chemistry is the most likely removal mechanism for α-terpineol. When compared to the pseudo-first order rate constants of the OH• ($k_{OH + \alpha\text{-terpineol}} = 190 \times 10^{-12}$ cm^3 $molecule^{-1}$ s^{-1}, $k' = 0.084$ h^{-1}) and ozone ($k_{O_3+\alpha\text{-terpineol}} = 3.0 \times 10^{-16}$ cm^3 $molecule^{-1}$ s^{-1}, $k' = 0.53$ h^{-1}), it is evident that nitrate radical chemistry plays a critical role in the transformation of α-terpineol in the indoor environment (Wells, 2005).

Nitrate radical reactions can lead to a number of organic nitrate products such as: peroxyacyl nitrates (PANs), alkyl nitrates, hydroxynitrates, and dinitrates (Muthuramu et al., 1993). Organic nitrates have received considerable interest because of their potential for deleterious health effects. For example, peroxyacetyl nitrate (PAN) has been shown in rats to induce respiratory tract damage in the form of chronic hyperplastic trachobronchitis, bronchiolitis, and pneumonitis. Furthermore, in some mice, trachea and mainstream bronchi also produce precancerous cells (Dungworth et al., 1969). However, only minimal toxicity data exists for alkyl and arylalkyl nitrates, hydroxynitrates and dinitrates. It is expected that these compounds may have harmful health effects and should be investigated. Nevertheless, predictions of organic nitrate hazards can be made using the Hazassess program developed by Jarvis et al. (Hazassess program, 2005; Jarvis et al., 2005). Using this program, 4HMON and 5HMON were determined to be "borderline hazardous", while DHDN was determined to be "undoubtedly hazardous". Although, this program should not be used to confirm the toxicity of these

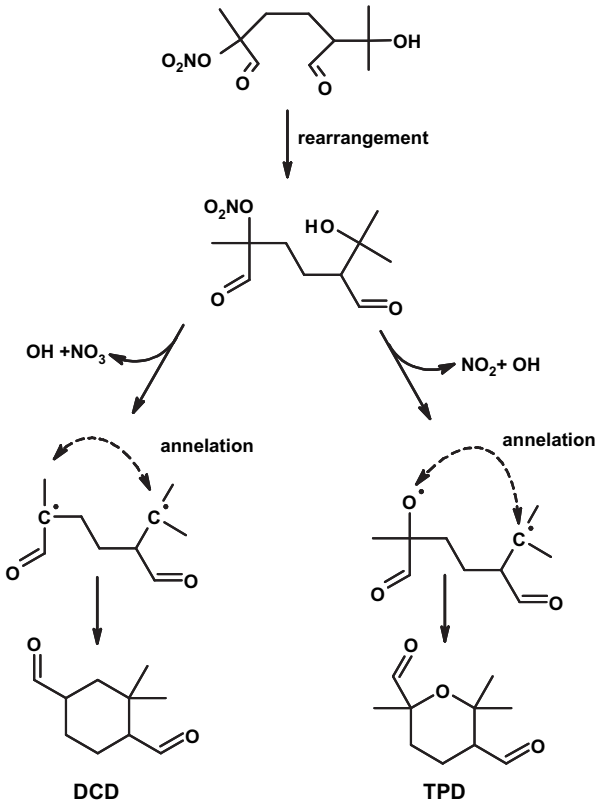

Fig. 7. Proposed reaction mechanism for α-terpineol + NO_3• showing the formation of 2,6,6-trimethyltetrahydro-2H-pyran-2,5-dicarbaldehyde (TPD) and 2,2-dimethylcyclohexane-1,4-dicarbaldehyde (DCD) from the organic nitrate, 1,4-diformyl-5-hydroxy-1,5-dimethylhexyl nitrate (DHDN).

compounds, it does give insight into potential factors that can affect indoor air quality.

Acknowledgements

The authors would like to thank J.R. Wells (National Institute for Occupational Safety and Health) and Charles Weschler (Environmental and Occupational Health Science Institute) for helpful discussions on nitrate radical indoor chemistry and reaction mechanisms.

Conflict of interest

The findings and conclusions in this report are those of the authors and do not necessarily represent the views of the National Institute for Occupational Safety and Health.

References

Anderson, S.E., Wells, J.R., Fedorowicz, A., Butterworth, L., Meade, B.J., Munson, A.E., 2007. Evaluation of the contact and respiratory sensitization potential of volatile organic compounds generated by simulated indoor air chemistry. Toxicol. Sci. kfm043.

Atkinson, R., 2000. Atmospheric oxidation. In: Boethling, R.S., Mackay, D. (Eds.), Handbook of Property Estimation Methods for Chemicals: Environmental and Health Sciences. Lewis Publishers, Boca Raton, pp. 335–354.

Atkinson, R., Arey, J., 2003. Atmospheric degradation of volatile organic compounds. Chem. Rev. 103, 4605–4638.

Atkinson, R., Aschmann, S.M., Pitts, J.N., 1988. Rate constants for the gas-phase reactions of the NO_3 radical with a series of organic compounds at 296 ± 2 K. J. Phys. Chem. 92, 3454–3457.

Atkinson, R., Plum, C.N., Carter, W.P.L., Winer, A.M., Pitts, J.N., 1984. Rate constants for the gas-phase reactions of nitrate radicals with a series of organics in air at 298 ± 1 K. J. Phys. Chem. 88, 1210–1215.

Brauer, M., Koutrakis, P., Keeler, G.J., Spengler, J.D., 1991. Indoor and outdoor concentrations of inorganic acidic aerosols and gases. J. Air. Waste. Manage. Assoc. 41, 171–181.

Dungworth, D.L., Clarke, G.L., Plata, R.L., 1969. Pulmonary lesions produced in a A-strain mice by long-term exposure to peroxyacetyl nitrate. Am. Rev. Respir. Dis. 99, 565–574.

EPA, 2006. U.S. sources of indoor air pollution – nitrogen dioxide (NO_2). Available from: <http://www.epa.gov/iaq/no2.html>.

Espada, C., Grossenbacher, J., Ford, K., Couch, T., Shepson, P.B., 2005. The production of organic nitrates from various antropogenic volatile organic compounds. Int. J. Chem. Kinet. 37, 675–685.

Finlayson-Pitts, B.J., Pitts, J.J.N., 2000. Chemistry of the Upper and Lower Atmosphere. Academic Press, New York.

Forester, C.D., Ham, Jason E., Wells, J.R., 2007. Geraniol (2,6-dimethyl-2,6-octadien-8-ol) reactions with ozone and OH radical: rate constants and gas-phase products. Atmos. Environ. 41, 1188–1199.

Ham, J.E., Proper, S.P., Wells, J.R., 2006. The gas-phase chemistry of citronellol with ozone and OH radical: rate constants and products. Atmos. Environ. 40, 726–735.

Hazassess program 2005. Edinburgh, UK. Available from: <http://homepages.ed.ac.uk/jjarvis/research/hazassess/hazassess.html> (accessed 13.11.2007).

Jarvis, J., Seed, M.J., Elton, R.A., Sawyer, L., Agius, R.M., 2005. Relationship between chemical structure and the occupational asthma hazard of low molecular weight organic compounds. Occup. Environ. Med. 62, 243–250.

Kames, J., Schurath, U., 1993. Preparation of organic nitrates from alcohols and N_2O_5 for specied identification in atmospheric samples. J. Atmos. Chem. 16, 349–359.

Muthuramu, K., Shepson, P.B., Obrien, J.M., 1993. Preparation, analysis, and atmospheric production of multifunctional organic nitrates. Environ. Sci. Technol. 27, 1117–1124.

Nazaroff, W.W., Weschler, C.J., 2004. Cleaning products and air fresheners: exposure to primary and secondary air pollutants. Atmos. Environ. 38, 2841–2865.

Rheault, T.R., Sibi, M.P., 2003. Radical-mediated annulation reactions. Synthesis (Stuttg) 6, 803–819.

Sarwar, G., Corsi, R., Kimura, Y., Allen, D., Weschler, C.J., 2002. Hydroxyl radicals in indoor environments. Atmos. Environ. 36, 3973–3988.

Semikolenov, V.A., Ilyna, I.I., Simakova, I.L., 2002. Effect of heterogeneous and homogeneous pathways on selectivity of pinane-2-ol to linalool isomerization. J. Mol. Catal. A Chem. 182, 383–393.

Shu, Y.H., Kwok, E.S.C., Tuazon, E.C., Atkinson, R., Arey, J., 1997. Products of the gas-phase reactions of linalool with OH radicals, NO_3 radicals, and O_3. Environ. Sci. Technol. 31, 896–904.

Skov, H., Hjorth, J., Lohse, C., Jensen, N.R., Restelli, G., 1992. Products and mechanisms of the reactions of the nitrate radical (NO_3) with isoprene, 1,3-butadiene and 2,3-dimethyl-1,3-butadiene in air. Atmos. Environ. 26A, 2771–2783.

Spittler, M., Barnes, I., Bejan, I., Brockmann, K.J., Benter, T., Wirtz, K., 2006. Reaction of NO_3 radicals with limonene and α-pinene: product and SOA formation. Atmos. Environ. 40, S116–S127.

Wells, J.R., 2005. Gas-phase chemistry of alpha-terpineol with ozone and OH radical: rate constants and products. Environ. Sci. Technol. 39, 6937–6943.

Weschler, C.J., Brauer, M., Koutrakis, P., 1992. Indoor ozone and nitrogen-dioxide–a potential pathway to the generation of nitrate radicals, dinitrogen pentaoxide, and nitric-acid indoors. Environ. Sci. Technol. 26, 179–184.

Weschler, C.J., Shields, H.C., 1997. Potential reactions among indoor pollutants. Atmos. Environ. 31, 3487–3495.

Weschler, C.J., Shields, H.C., Naik, D.V., 1994. Indoor chemistry involving O_3, NO and NO_2 as evidenced by 14 months of measurements at a site in Southern California. Environ. Sci. Technol. 28, 2120–2132.

Wilson, A.L., Colome, S.D., Tian, Y., Becker, E.W., Baker, P.E., Behrens, D.W., Billick, I.H., Garrison, C.A., 1996. California residential air exchange rates and residence volumes. J. Expo. Anal. Environ. Epidemiol. 6, 311–326.

Woidich, S., Froescheis, O., Luxenhofer, O., Ballschmiter, K., 1999. EI- and NCl-mass spectrometry of arylalkyl nitrates and their occurrence in urban air. Fresenius J. Anal. Chem. 364, 91–99.

Yu, J.Z., Flagan, R.C., Seinfeld, J.H., 1998. Identification of products containing -COOH, -OH, and -CO in atmospheric oxidation of hydrocarbons. Environ. Sci. Technol. 32, 2357–2370.